



## Molecular Structure, Thermochemistry, Non-Covalent Interactions Computation Using DFT Studies Of The 1 Amino 2-(3,4- Dihydroxyphenyl) Boronic Acid (AHPEBA) Compound

 *Rebaz Obaid Kareem*

*Physics Department, College of Science, University of Halabja, 46018, Halabja, Iraq*

*\*Corresponding author: E-mail: rebaz.kareem@uoh.edu.iq*

### ABSTRACT

Theoretical parameters for 1 amino 2-(3,4- dihydroxyphenyl) boronic acid in AHPEBA were investigated using density functional theory (DFT), and STO-3G basis set. Quantum chemical calculations were done on the link between inhibitor molecular structure, chemical reactivity, stability, and inhibition performance. In addition, we investigate the theoretical foundations of AHPEBA by looking at properties and characteristics such as the Highest Occupied Molecular Orbital (HOMO), the Lowest Unoccupied Molecular Orbital (LUMO), the Band Gap (BG), the Density of States (DOS), the Ultraviolet (UV) properties, and the Natural Bond Orbital (NBO) evaluations. Also, we use the reduced density gradient (RDG) method to explore non-covalent interactions (NCI). The fact that the BG was measured to be -5.85043 eV lent credence to the hypothesis that the molecule had a high level of chemical stability and a low level of chemical reactivity. According to molecular hardness and softness, electronegativity, and chemical potential, the molecule  $C_8H_{12}BNO_4$  has a high degree of chemical stability, and a low degree of reactivity. This is the first theoretical study of the AHPEBA compound.

### ARTICLE INFO

*Keywords:*

*AHPEBA compound  
NCI  
RDG  
FTIR  
UV spectroscopy  
Thermochemistry  
HOMO-LUMO*

**Received:** 2023-11-24

**Accepted:** 2024-02-16

**ISSN:** 2651-3080

**DOI:** 10.54565/jphcfum.1395735

### 1. Introduction

The chemical compound are referring to, "1 amino 2-(3,4- dihydroxyphenyl) boronic acid.". The short name of 1 amino 2-(3,4- dihydroxyphenyl) boronic acid is AHPEBA. The AHPEBA has the chemical formula  $C_8H_{12}BNO_4$  according to its molecular structure. AHPEBA is more commonly known as "L-DOPA boronic acid" or "Levodopa boronic acid." This compound is a derivative of Levodopa, which is a medication commonly used to treat Parkinson's disease. Levodopa is converted into dopamine in the brain, helping to alleviate the symptoms of Parkinson's disease, which is characterized by a deficiency of dopamine. The boronic acid derivative you mentioned likely contains a boron atom attached to the phenyl ring of the L-DOPA molecule. The boronic acid group can form reversible bonds with certain molecules and may have applications in chemical reactions or pharmaceutical research [1, 2].

The compound mentioned is Here's a breakdown of the compound's name: "Amino" indicates the presence of an amino group ( $NH_2$ ) in the molecule. "2-(3,4-dihydroxyphenyl)" specifies the substitution on the boronic acid core, with two hydroxy groups (OH) attached to the 3rd and 4th positions of a phenyl ring. "Boronic acid" refers to the boron-containing acid functional group ( $B(OH)_3$ ) in the compound [3]. To impart distinct adsorption capabilities onto the magnetic nanoparticles, different functional groups have been used. Adsorption selectivity results from the interaction of analytes with the functional groups on the surface of adsorbents. Since boronic acids can form covalent bonds with cis-diols in alkaline solution to generate five- or six-membered cyclic esters that can reversibly disassociate under acidic conditions, they are well-suited for functionalizing different matrices for the specific capture of cis-diol-containing molecules from complex samples. The AHPEBA chemical has been used in the manufacture of boronic-acid-labeled thymidine triphosphate for integration into DNA. Additionally, it has been utilized for

the production of imidazo[1,2-a] quinoxaline derivatives that have been grafted with amino acids [2, 4, 5]. Certain types of boronic acids, however, are notoriously prone to breakdown, rendering them ineffective in coupling processes or making long-term storage problematic. In addition, the high reactivity of boronic acids prevents repetitive Suzuki Miyaura cross-couplings from being performed under moderate circumstances, which limits their use in the synthesis of small compounds [6].

Applications such as solid-phase metal extraction, hybrid organic-inorganic catalysts, and hydrogenizing homogeneous catalysts have kept researchers interested in ligand-immobilized solid phases such as silica gel, organic polymer or copolymers, and cellulose. Therefore, chelating resin with very high capacity may be anchored from a multidentate ligand, such as 1 amino 2-(3-hydroxyphenyl) boronic acids [7]. The boronic acid group may be put to use in a variety of contexts due to its ability to recognize carbohydrates, bind to glycoproteins, block hydrolytic enzymes, and trap boron neutrons. Boronic acid might be incorporated into DNA to create molecules with new biological properties. Biological receptors are typically big protein structures that recognize and bind to certain ligands. The amino acid residues and other species, such as metal ions, that make up a protein's binding site have evolved to form highly specialized, frequently extremely strong interactions with their target molecule, making them valuable biochemical instruments [8, 9]. The incorporation of boron acid into DNA has the potential to result in the production of molecules that possess distinctive biological properties. Large protein structures that are able to detect and bind to certain ligands are those that are known as biological receptors. The amino acid residues and other species that make up a protein's binding site have become more robust, allowing them to create highly specialized and often forceful interactions with their target molecule. As a result, these proteins have become important biochemical instruments [8, 9].

This is the first theoretical study of the AHPEBA ( $C_8H_{12}BNO_4$ ) compound. The DFT/STO-3G method was performed when used to estimate the structure of the molecule. Among the many parameters that have been investigated in this current work are NMR, UV, DOS, NCI, REG, and thermochemistry.

## 2. Computational Method

For all of the essential atomic calculations and simulations in the three-dimensional form of the molecule components, while they were in the gas phase, the computer program Gaussian 5.0.9W was used as the primary tool. The program known as the Gauss View 5.0 package was used, and the Gaussian 09W was used, to identify the starting geometries of the compounds. The output calculations were done using the Gaussian 09W [10]. The DFT approach can produce the required output data for a more accurate calculation of the electronic characteristics of complex structures because it takes into consideration the density of electrons. DFT is now the most extensively utilized technique since it produces realistic and reliable findings [11, 12].

In addition, DFT is one of the significant techniques that has been shown to have a significant advantage over Hartree-Fock. Using structures with optimized forms for

computation. The following qualities have their respective parameters calculated:  $E_{LUMO}$ ,  $E_{HOMO}$ , total energy  $\Delta E$ , electronegativity ( $\chi$ ), hardness ( $\eta$ ), softness ( $\sigma$ ), electrophilicity index ( $\omega$ ), nucleophilicity index ( $\epsilon$ ), Chemical potential ( $P_i$ ), and dipole moment ( $\mu$ ) [13-16]:

Neutrality is the difference between IE and EA, or cation and anion. By solving equations (1) and (2), we calculated ionization energy and electron affinity [13, 17-19]:

$$(1)$$

And

$$(2)$$

Here we designate the energy (E) of the neutral by (N), that of the cation by (N-1), and that of the anion by (N+1). The band gap energy ( $E_{gap}$ ) is the energy difference between  $E_{LUMO}$  and  $E_{HOMO}$ , as stated in equation (3) [13]:

$$(3)$$

For the computation, equation (4) was used. This allowed for the determination of the absolute chemical hardness [13]:

$$\eta = \frac{IE - EA}{2} = \frac{E_{HOMO} - E_{LUMO}}{2} \quad (4)$$

The molecular softness of an atom or collection of atoms is characterized by the electron-receiving regions, as shown in equation (5) [13]:

$$S = \frac{1}{\eta} = \frac{2}{E_{LUMO} - E_{HOMO}} \quad (5)$$

As can be observed in equation (6), the negative value of the chemical potential makes a considerable contribution to the overall reactivity [13]:

$$\chi = \frac{IE + EA}{2} = \frac{-(E_{HOMO} + E_{LUMO})}{2} \quad (6)$$

To get the electronic chemical potential using electronic molecular orbital (EMO) energies, we utilize the following formula (7):

$$\mu = \frac{E_{HOMO} + E_{LUMO}}{2} \quad (7)$$

With the support of equation (8), we were able to determine how much of an energy loss resulted from the transfer of electrons from the donor to the acceptor. In addition, the electrophilicity ( $\omega$ ) index of a chemical species may be calculated by squaring its electronegativity ( $\chi$ ) and then multiplying the result by its chemical hardness. This definition was provided by Parr and colleagues [16, 17]:

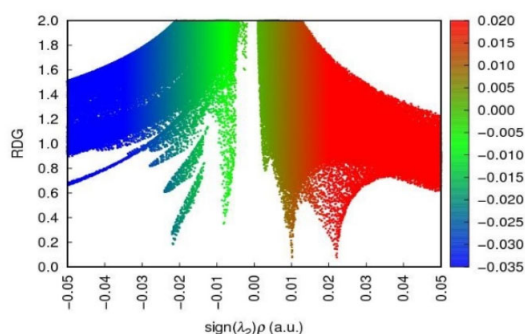
(8)

Equations (9) and (10) were used to calculate the number of provided and obtained electrons [13, 20]. Where  $(\omega^+)$  denotes that the system may accept charges from other molecules and  $(\omega^-)$  suggests that it can release charges to other compounds:

$$\omega^+ = \frac{EA^2}{2(IE - EA)} \quad (9)$$

$$\omega^- = \frac{IA^2}{2(IE - EA)} \quad (10)$$

We find that systems with larger values for  $(\omega^+)$  may get charged, whereas those with smaller values for  $(\omega^-)$  are more efficient electron donors. Using the quantum chemical technique, we have utilized the following equation (11) to determine the maximum number of electrons that an electrophile might receive. [13]:



(11)

In this study, atom-by-atom calculations and molecular-level simulations were carried out in the gas phase using the software package Gaussian 5.0.9W. In addition to energy, which may be calculated in a variety of methods, it can be used to establish other molecular characteristics, such as vibrational wave numbers [21]. Some examples of experimental and theoretical approaches to studying molecular structure and properties include nuclear magnetic resonance (NMR) spectra, ultraviolet (UV) spectra, and Fourier transform infrared (FTIR) spectra. NMR spectroscopy may be used to determine the molecular weight, atomic composition, and atomic bonding of a given molecule [22]. Ultraviolet (UV) spectroscopy may be used to determine the electrical configuration of an element. FTIR spectroscopy may be used to determine the vibrational frequencies of a substance. The Gauss Sum program makes it easy to determine a molecule's DOS spectrum. The energy versus the number of states shown on a diagram is called the

density of states (DOS) spectrum. It may be used to get insight into a molecule's vibrational modes and the relative energies of those modes [23].

### 3. Result and Discussion

#### 3.1 Geometry Optimization

Running the Gaussian program in combination with the DFT/ ST0-3G basis and setting it to the structure of the AHPEBA molecule resulted in the optimal form, as illustrated in Figure 1. Molecules have their unique orbitals, which are separate from the orbitals that are present in atoms. The first stage of an approach to geometry optimization that is helpful for this method centers on the energy that is associated with a certain starting molecule shape. This energy is the focus of the first step. It has been shown that AHPEBA has the best geometrical optimization. The chemical and biological activity of organic compounds is directly proportional to the geometry of their molecular orbitals, in addition to the nature of the orbitals themselves [24].

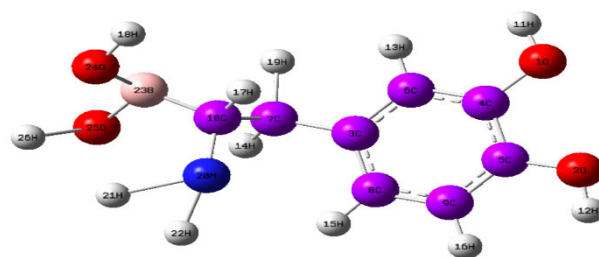


Figure 1. Geometrical optimization AHPEBA molecule

Conversely, the imaginary frequency for transition structure is negative, confirming that these structures are transition state structures [10, 25].

#### 3.2 NCI, RDG Techniques

Two new techniques for studying weak intermolecular interactions are reduced density gradient (RDG) approaches and non-covalent interactions (NCI). RDG is an effective technique for researching noncovalent interactions in real space, and it depends on the density of electrons (DOE), and its derivatives. It has been shown that this method can differentiate between Figure 2 shows the expected RDG plots hydrogen bonds, van der Waals interactions, and electrostatic attraction in complex molecular systems and tiny molecules. The following equation (12) was what we utilized to compute the RDG values [26-28]:

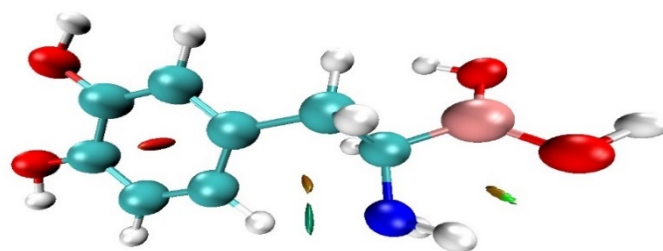


Figure 3. The NCI, and RDG AHPEBA molecule

$$RDG(r) = \frac{1|\nabla\rho(r)|}{2(3\pi r^2)^{\frac{1}{3}}\rho^{\frac{4}{3}}(r)} \quad (12)$$

It is possible to validate the existence of areas with a low electron content, which is the cause of weak interactions, by an examination of the low-density gradient. Comparably, the high-density gradient value is used to locate strong interactions. The values shown in Bellow Figures 2, and 3 of RDG, and NCI against (low-gradient peak density values) seem to be a measure of the magnitude of an interaction. It has been suggested that one may differentiate between a large variety of interaction types by using a tool that is composed of the product of the electron density, and the sign of the second eigenvalues  $\lambda_2$ . The sign  $\lambda_2$  is an important characteristic that is used to differentiate between bound interactions ( $\lambda_2 < 0$ ) and non-coupling interactions ( $\lambda_2 > 0$ ) [27].

Interactions may be broken down into three distinct categories according to the formula  $(\lambda_2)\rho$ : i) The first kind is an attraction, often known as a hydrogen bond or a dipole-dipole interaction, and it is denoted by numbers with a negative sign ( $\lambda_2\rho$ ); ii) The second model implies a nonbinding interaction of a very powerful repulsion type, which is supported by high and positive values of the sign ( $\lambda_2\rho$ ). This interaction is nonbinding and of the strong repulsive sort; iii) The third category, known as weak contacts (also known as van der Waals interactions), is connected to values that are almost near to zero [26, 27]. Figure 2 shows the expected RDG plots for the AHPEBA compound. The color red denotes the existence of strong intermolecular interactions. The second one, which was colored green, demonstrated the van der Waals interaction. The third, represented by the color blue, indicated the presence of strong hydrogen bond interactions of 1 amino 2-(3,4- dihydroxyphenyl) boronic acid molecules. The significant incidence of van der Waals contacts and the observed steric effect within the molecule may be responsible for these visible properties. Steric effects might have an important part. On the other hand, the green isosurface is representative of van der Waals (vdW) interactions, which include hydrogen-hydrogen (H-O), nitrogen-hydrogen (N-H), and oxygen-sulfur (O-B) pairings. These interactions demonstrate hydrogen bonding and other related interactions that are slightly weaker.

**Figure 4.** FT-IR Vibrational Spectroscopic AHPEBA compound

### 3.3 FT-IR Vibrational Spectroscopic Analysis

Using the DFT approach using the basis set STO-3G, we were able to make predictions about the vibrational frequencies of our materials for the C-C, H-H, N-H, and C-B, as shown in Figure 4. The results of the infrared examinations performed on the AHPEBA compound are shown here. The results of the IR analysis revealed the following FT-IR spectra for this compound: C-H asymmetric stretching vibration peak for the structure occurred at ( $3519.76 \text{ cm}^{-1}$ ), and Asymmetric-Bending at ( $1369.12 \text{ cm}^{-1}$ ); C-H<sub>2</sub> ( $1401.10 \text{ cm}^{-1}$  Asymmetric -Bending), and Asymmetric -Bending at ( $1280.31 \text{ cm}^{-1}$ ); C-N ( $193.46 \text{ cm}^{-1}$  Vibrational Bending); C-C ( $1401.10 \text{ cm}^{-1}$  vibrational bending); Benzin ring in the range between ( $1401.10$  to  $1779.00 \text{ cm}^{-1}$ ) Vibrational Stretching, as shown in the bellow Table 1.

The temperature may influence the intensity, width, and location of the absorption bands. The peak was detected in the FT-IR spectra at  $4200 \text{ cm}^{-1}$ . The asymmetric O=H vibration (stretching) is  $4240 \text{ cm}^{-1}$ , whereas the symmetrical vibration is  $4247 \text{ cm}^{-1}$ . Temperature fluctuations may have an impact on the stability of FTIR spectrometers [29].

### 3.4 Natural Bond Orbital (NBO) Analysis

After optimizing the molecular structures of substituted arynes using DFT calculations, build the electron density model by utilizing the natural bond orbital (NBO) approach. These values do not signify charge; rather, they indicate the electron density of each orbital [30]. When trying to characterize the activity of a chemical, one of the crucial factors that has to be taken into consideration is the assignment of atomic charges, as seen in Figure 5. The pH of the solution affects the charge that is carried by the AHPEBA molecule. The molecule has no net charge at physiological pH (which is about 7.4). The amino group is protonated, but the boronic acid group is deprotonated, and this is the reason for this behavior. There is both a positive and a negative charge, as seen in Figure 6. A lower pH allows the boronic acid group to get protonated, which results in a positive charge being given to the molecule. A higher pH may cause the amino group to get deprotonated, which results in a negative charge being added to the molecule.

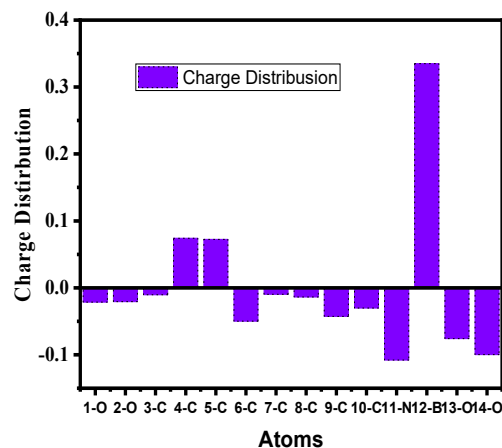


**Figure 5.** Mulliken charges with hydrogens summed into heavy atoms

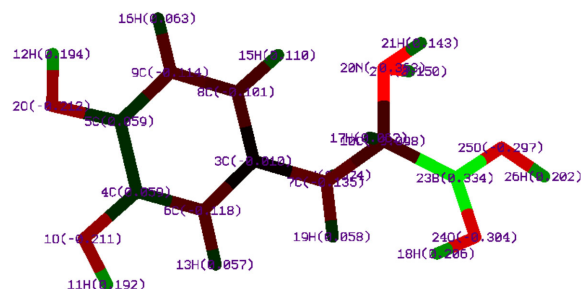


**Figure 6.** NBO Analysis of AHPEBA compound with different color

The AHPEBA molecule is a very complex chemical compound. For instance, the charge of the chemical may influence how well it dissolves in water, how well it interacts with other molecules, and how active it is

biologically. Molecules' colors are mostly dictated by the wavelengths of light absorbed by their electrons. Electrons interacting with visible light photons create the color. Because oxygen is so much more electronegative than hydrogen or carbon, polar bonds may form between the two elements. Carbon and hydrogen are somewhat positively charged, whereas oxygen is slightly negatively charged [31]. The electronegativity of a functional group or atomic structure is the degree to which it attracts electrons. The electronegativity  $O(3.5) > N(3.04) > B(2.04) > H(2.02)$  [32, 33]. As shown in Figure 5, Oxygen charge  $> N, B, C, H$  atoms. This is because influences electronegativity.

### 3.5 UV-Visible Analysis

To optimize the ground-state electron configuration of the AHPEBA molecule. The electronic excitation in the low energy state is estimated using the DFT method at the (B3LYP/STO-3G basis set). According to DFT calculations, there is just one transition in the invisible region of electromagnetic radiation. The kind of basis set used is more important than the number of peaks when determining how accurately UV-visible wavelengths can be calculated. The of both transitions and absorptions [34]. In this study, the maximum wavelength investigated at 802 nm, and 0.0031 oscillator strength. The  $\lambda_{max}$  is denoted as the longest visible light wavelength at which the molecule or atom absorbs significant amounts of energy. In Figure 7, the  $\lambda_{max}$  is an important parameter because it specifies the nature of the electronic transition taking place in the molecule. Maximum absorption wavelength coincides with the HOMO-LUMO electronic transition, as seen by the spectra

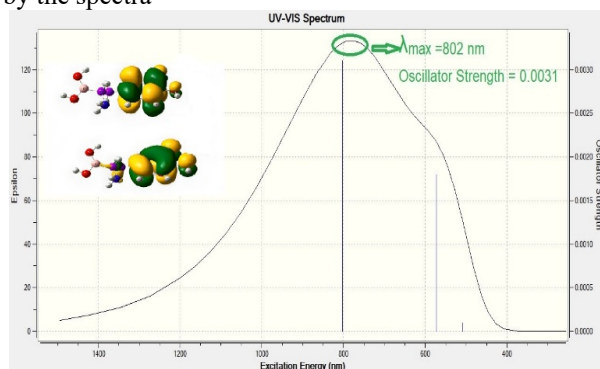


**Figure 7.** UV-Visible analysis of AHPEBA molecule

### 3.5 Thermochemistry

This study used DFT and the STO-3G basis to estimate the thermodynamic property characteristics of this chemical at various temperatures (100, 150, 200, and 250 K). The results of this research are shown in Table 2. These properties of thermodynamic belongings include thermal energy (E), molar heat capacity (Cv), and entropy (S) [35].

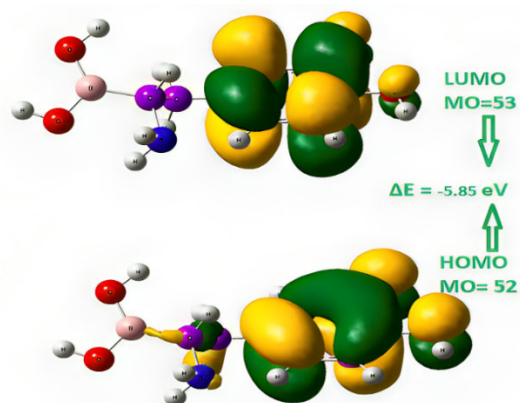
The energy that is maintained by an item or system as a result of its temperature is referred to as its thermal energy [36]. As demonstrated in Table 2, and Figure 10, the sum of the contributions from translation ( $E_{trans}$ ), rotation ( $E_{rot}$ ), and vibration ( $E_{vib}$ ), translation ( $CV_{trans}$ ), rotation ( $CV_{rot}$ ), and vibration ( $CV_{vib}$ ), and translation ( $S_{trans}$ ), rotation ( $S_{rot}$ ), and vibration ( $S_{vib}$ ) were used to calculate the total thermal energy, entropy, and heat capacity [35].

Figure 10 illustrates how the total energy, entropy, and heat capacity of the AHPEBA molecule changes as a function of temperature. Utilizing this information, a prediction of the CV, S, and E of the materials was created for the temperature range that was provided [35]. First, let's investigate the energy of rotation. The lowest possible change in a spinning system's angular momentum, as determined by quantum physics, is given by  $\Delta L = h/2\pi$ , where h is Planck's constant. Figure 10a-c red curve displays the AHPEBA compound's computed CV as a function of temperature. This result indicates the amount of energy required to heat or cool the chemical [37]. According to Table 2, total thermal energy increased from 116.386 to 120.183 kcal/mol with temperature, and  $E_{vib}$  gradually increased from 115.790 to 118.692. However,  $E_{rot}$  is too tiny when compared to  $E_{total}$ . Due to translation energy being greater than that of  $E_{rot}$  and  $E_{vib}$ . Total CV is greater than vibrational and rotational CV because translational CV is associated with particle motion overall, whereas vibrational and rotational CV are associated with molecular mobility.

In conclusion, the molecule structure and the temperature range of interest determine how important the vibrational and rotational contributions are to one other. When thermal energy is limited at extremely low temperatures, rotational contributions may account for the majority of the heat capacity. The significance of vibrational, and rotational modes grows with temperature.

### 3.5 Computed Electron Structure

The difference in energy level between  $E_{HOMO}$  and  $E_{LUMO}$  influences both the theoretical efficacy of inhibitors and the static molecular reactivity of molecules. The difference in potential energy that exists between the HOMO and LUMO states of a molecule is referred to as the (BG) energy of the molecule. As can be seen in **Figure 8**, throughout our investigation, we analyzed the performance of STO-3Gsets of basis at an extensive spectrum of BG energy levels [13, 38]. The HOMO and LUMO energies were initially calculated using DFT/ STO-3G basis sets, as shown in **Table 3**.



**Figure 8.** The HOMO, and LUMO of AHPEBA molecule, B3LYP/ DFT/ STO-3G basis set

**Table 3.** Molecular parameters of AHPEBA molecule parameters

Electronic Computation DFT/STO-3G			
$E_{HOMO}$ (eV)	-3.07488	$\chi$ (eV)	1.687101

$E_{LUMO}$ (eV)	2.77553	$\omega$ (eV)	0.486513
$\Delta E$ (eV)	-5.85043	$\epsilon$ (Pi) (eV)	-1.6871
IE	3.074877	$\omega^+$ (eV)	0.658387
EA	-2.77555	$\omega^-$ (eV)	0.808049
$\eta$ (eV)	2.925215	$\mu$ (C.m)	0.149662
$\sigma$ (eV <sup>-1</sup> )	0.341855	$\Delta N_{max}$	-0.05116

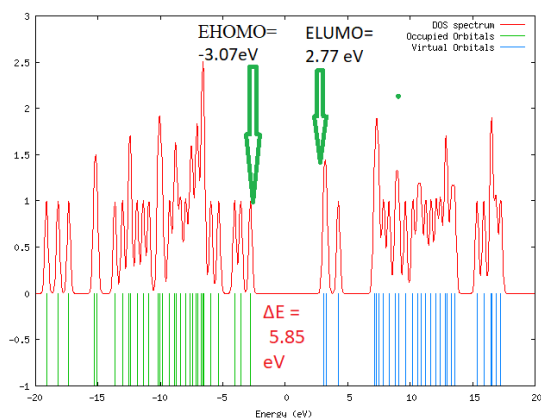


**Figure 9.** DOS for AHPEBA compound, with STO-3G basis set, and B3LYP

The calculations for density of state (DOS) were described in more depth in several earlier papers. In a quantum mechanical system, the electronic DOS is a measurement that determines how "packed" electrons are at different energy levels as shown above in Figure 9 [39–42]. The DOS makes it possible to determine the quantity of electrons present in each energy level, and the diagram of these states contradicts the idea that a material may transmit electricity. Through the mechanism of charge transfer, they hypothesized that the chemical potential plays a significant part in the explanation of chemical processes [43, 44]. The difference in energy level that exists between the HOMO and LUMO orbitals is a big value to allow for the study of the (C<sub>8</sub>H<sub>12</sub>BNO<sub>4</sub>) molecule's stability as well as its chemical reactivity. The capacity to provide electrons is denoted by the HOMO energy, while the ability to absorb electrons is denoted by the LUMO energy. The difference in energy levels between HOMO and LUMO orbitals is what determines the chemical stability, optical polarizability, and chemical reactivity of a molecule. The value of the energy gap is high, which suggests that this molecule has a higher degree of stability. Molecules having low HOMO–LUMO energy gaps tend to be more reactive, or (soft). The difficulty of the molecule represented by the formula (C<sub>8</sub>H<sub>12</sub>BNO<sub>4</sub>) is exactly related to the energy gap ( $I \propto E_g$ ) [45]. Ionization potential (IA) is a measure of a compound's ability to lose electrons, while electronic affinity (EA) is a measure of the compound's capacity to acquire valence electrons. Both of these properties are measured using the electron ionization model. The greater value of the IA parameter indicates that it is difficult to remove an electron to create an ion, while the higher value of the EA parameter in a molecule shows that it is difficult to add an electron to the molecule. On the other hand, the electron affinity must be lower before an ion may be

created by the addition of an electron. This makes the process easier. In the quantum chemical process, two crucial characteristics are electronegativity and the electronic chemical potential [45].

When the value of electronegativity is high, atoms and molecules have a larger capacity to attract electrons. On the other hand, when the value of chemical potential is high, there is more reactivity and less stability. This molecule exhibits a small electronegativity of 1.6871 eV and a chemical potential of -1.6871 eV when it is dissolved in water. According to these observations, the molecule with the formula (C<sub>8</sub>H<sub>12</sub>BNO<sub>4</sub>) has a low capacity to attract electrons and a low level of reactivity. Because of this, it can be deduced that the compound with the formula C<sub>8</sub>H<sub>12</sub>BNO<sub>4</sub> has a high degree of chemical stability and a low degree of reactivity. Absolute hardness is a crucial quality to have when one is thinking about the structural stability and reactivity of a material. Because they can give up electrons more easily, soft compounds are more reactive than hard ones. As a result, we estimate that the inhibitors with the lowest global hardness values will be effective corrosion inhibitors [45, 46].

The dipole moment ( $\mu$ ) measurements are summarised in Table 3. There is no correlation found in previous research between  $\mu$  and inhibitory activity. In several investigations, the molecules' activity grew as the  $\mu$  value increased whereas in other investigations, the activity of the inhibitory molecule reduced as the  $\mu$  value increased [46]. It is crucial to consider the electrophilicity index ( $\omega$ ) and nucleophilicity index ( $\epsilon$ ) when identifying factors that inhibit corrosion activity, chemical stability, and selectivity. The value of  $\omega$  indicates the electron-accepting capability of the inhibitor molecules, whereas  $\epsilon$  indicates their electron-donating capability. When compared to a powerful electrophile with a high value of ( $\omega$ ), a more reactive nucleophile will have a value of that parameter that is lower ( $\omega$ ). A positive transmission number ( $\Delta N$ ) indicates that the atoms are providing electrons. On the other hand, substances that have a negative value of ( $\Delta N$ ) are electron acceptors. The efficacy of the inhibition is increased by increasing the inhibitor's ability to donate electrons at the molecular surface if ( $\Delta N$  is less than 3.6) [46].

Overall, the link between inhibition, chemical reactivity, and stability is a complicated issue. Fewer reactive properties are associated with more stable compounds. This is because stable compounds have a lower energy state, and for them to respond, they need to absorb energy. On the other hand, less stable substances tend to be more reactive because they are in a higher energy state and because they may release energy via the process of responding.

**Table 1.** The characteristic FTIR spectrum for AHPEBA compound, temperature=150 K, 1 atm pressure

Peaks (cm <sup>-1</sup> )	Chemical compound	Vibrational mode	Peaks (cm <sup>-1</sup> )	Chemical compound	Vibrational mode
1214.92	C-H	Symmetric-Bending	1401.10	C-C	Vibrational Bending
1369.12	C-H	Asymmetric-Bending	527.21	O-H	Asymmetric - Bending
3519.76	C-H	Asymmetric - Stretching	4240.57	O-H	Asymmetric - Stretching
1280.31	C-H <sub>2</sub>	Asymmetric - Bending	2968.69	O-H	Vibrational Stretching
1401.10	C-H <sub>2</sub>	Symmetric - Bending	1401.10	Benzene Ring	Vibrational Stretching
193.46	C-N	Vibrational Bending	1779.00		

**Table 2.** Influence of different temperatures, constant pressure at 1 atm for AHPEBA compound

Temperature (K)	Total			Rotational			Vibrational		
	E kcal/mol	Cv cal/mol.K	S cal/mol.K	E kcal/mol	Cv cal/mol.K	S cal/mol.K	E kcal/mol	Cv cal/mol.K	S cal/mol.K
100	116.386	15.145	70.151	0.298	2.981	36.313	115.790	9.183	4.877
150	117.304	21.666	78.316	0.447	2.981	30.170	116.410	15.704	9.818
200	118.562	28.706	86.071	0.596	2.981	31.027	117.369	22.744	15.287
250	120.183	36.193	93.719	0.745	2.981	31.692	118.692	30.231	21.161

**Figure 10.** Thermochemistry investigation using various temperature, and constant pressure (1 atm)

## 5. Conclusions

In this current research, some of the physical and chemical behavior of 1 amino 2-(3,4- dihydroxyphenyl) boronic acid (AHPEBA,  $C_8H_{12}BNO_4$ ) compound. including (HOMO, LUMO, DOS, UV, IR spectra, potential energy map, NBO, RDG, NCI), and thermochemistry, has been explored. This investigation was carried out with the help of the Gaussian 5.0 program and the DFT/ STO-3G technique. C-H asymmetric stretching vibration peak for the structure occurred at ( $3519.76\text{ cm}^{-1}$ ), and Asymmetric-Bending at ( $1369.12\text{ cm}^{-1}$ ); C-H2 (  $1401.10\text{ cm}^{-1}$  Asymmetric -Bending), and Asymmetric -Bending at ( $1280.31\text{ cm}^{-1}$ ). In the UV study, the maximum wavelength investigated at 802 nm, and 0.0031 oscillator strength. In the thermochemistry calculation,  $E_{rot}$  is too small when compared to  $E_{total}$ . Due to translation energy being greater than that of  $E_{rot}$  and  $E_{vib}$ . The 3.074877 eV is the value of the IE compound that was studied. According to the higher value of the IA parameter, it is harder to remove an electron to produce an ion. The fact that the BG was measured to be -5.85043 eV suggested that the molecule has a high degree of chemical stability and a low degree of chemical reactivity.

## References

- [1] Ueno, H., Iwata, T., Koshiba, N., Takahashi, D. And Toshima, K., 2013. Design, Synthesis And Evaluation Of A Boronic Acid Based Artificial Receptor For L-DOPA In Aqueous Media. *Chemical Communications*, 49(88), Pp.10403-10405.
- [2] Enquiry.(2005).(1-Amino-2-(3,4-Dihydroxyphenyl)Ethyl)Boronic Acid ,95% Min., *Hairui Chemical*.
- [3] Pantalone, S., 2022. Food Contaminants Due To Thermal Process.
- [4] Du, J., He, M., Wang, X., Fan, H. And Wei, Y., 2015. Facile Preparation Of Boronic Acid-Functionalized Magnetic Nanoparticles With A High Capacity And Their Use In The Enrichment Of Cis-Diol-Containing Compounds From Plasma. *Biomedical Chromatography*, 29(2), Pp.312-320.
- [5] Chouchou, A., Patinote, C., Cuq, P., Bonnet, P.A. And Deleuze-Masquéfa, C., 2018. Imidazo [1, 2-A] Quinoxalines Derivatives Grafted With Amino Acids: Synthesis And Evaluation On A375 Melanoma Cells. *Molecules*, 23(11), P.2987.
- [6] Cross-Coupling, I. And Boronates, M.I.D.A., MIDA-Protected Boronate Esters.
- [7] Venkatesh, G. And Singh, A.K., 2005. 2-{{[1-(3, 4-Dihydroxyphenyl) Methylidene] Amino}}

- Benzoic Acid Immobilized Amberlite XAD-16 As Metal Extractant. *Talanta*, 67(1), Pp.187-194.
- [8] Lin, N., Yan, J., Huang, Z., Altier, C., Li, M., Carrasco, N., Suyemoto, M., Johnston, L., Wang, S., Wang, Q. And Fang, H., 2007. Design And Synthesis Of Boronic-Acid-Labeled Thymidine Triphosphate For Incorporation Into DNA. *Nucleic Acids Research*, 35(4), Pp.1222-1229.
- [9] Whyte, G.F., Vilar, R. And Woscholski, R., 2013. Molecular Recognition With Boronic Acids—Applications In Chemical Biology. *Journal Of Chemical Biology*, 6, Pp.161-174.
- [10] Ferreira, O.O., Mali, S.N., Jadhav, B., Chtita, S., Kuznetsov, A., Bhandare, R.R., Shaik, A.B., Siddique, F., Yadav, A.R., Lai, C.H. And Cruz, J.N., 2023. Synthesis, In-Silico, In Vitro And DFT Assessments Of Substituted Imidazopyridine Derivatives As Potential Antimalarials Targeting Hemoglobin Degradation Pathway. *Journal Of Computational Biophysics And Chemistry*, 22(7), Pp.795-814.
- [11] Rhazi, Y., Chalkha, M., Nakkabi, A., Hammoudan, I., Akhazzane, M., Bakhouch, M., Chtita, S. And El Yazidi, M., 2022. Novel Quinazolinone–Isoxazoline Hybrids: Synthesis, Spectroscopic Characterization, And DFT Mechanistic Study. *Chemistry*, 4(3), Pp.969-982.
- [12] Hammoudan, I., Chtita, S. And Riffi-Temsamani, D., 2020. QTAIM And IRC Studies For The Evaluation Of Activation Energy On The C= P, C= N And C= O Diels-Alder Reaction. *Heliyon*, 6(8).
- [13] HAMAD, O., KAREEM, R.O. And Kaygili, O., 2023. Density Function Theory Study Of The Physicochemical Characteristics Of 2-Nitrophenol. *Journal Of Physical Chemistry And Functional Materials*, 6(1), Pp.70-76.
- [14] Koohi, M. And Bastami, H., 2023. Investigation Of Ti—B Nanoheterofullerenes Evolved From C20 Nanocage Through DFT. *Chemical Review And Letters*, 6(2), Pp.223-234.
- [15] Azeez, Y.H., Kareem, R.O., Qader, A.F., Omer, R.A. And Ahmed, L.O., 2024. Spectroscopic Characteristics, Stability, Reactivity, And Corrosion Inhibition Of AHPE-Dop Compounds Incorporating (B, Fe, Ga, Ti): A DFT Investigation.
- [16] Rasul, H.H., Mamad, D.M., Azeez, Y.H., Omer, R.A. And Omer, K.A., 2023. Theoretical Investigation On Corrosion Inhibition Efficiency Of Some Amino Acid Compounds. *Computational And Theoretical Chemistry*, P.114177.
- [17] El Idrissi, M., Elharfaoui, S., Zmirli, Z., Mouhssine, A., Dani, A., Salle, B., Tounsi, A., Digua, K., And Chaair, H. (2024). Theoretical And Experimental Study Of The Orientation To The Most Effective Coagulant For Removing Reactive Black-5 Dye From Industrial Effluents, *Physical Chemistry Research*, 12 (1), Pp: 229-248.
- [18] Mamand, D.M., Azeez, Y.H. And Qadr, H.M., 2023. Monte Carlo And DFT Calculations On The Corrosion Inhibition Efficiency Of Some Benzimide Molecules. *Mongolian Journal Of Chemistry*, 24(50), Pp.Xx-Xx.
- [19] Hussein, Y.T. And Azeez, Y.H., 2023. DFT Analysis And In Silico Exploration Of Drug-Likeness, Toxicity Prediction, Bioactivity Score, And Chemical Reactivity Properties Of The Urolithins. *Journal Of Biomolecular Structure And Dynamics*, 41(4), Pp.1168-1177.
- [20] Kebiroglu, H., Hamad, O.A., Kaygili, O. And Bulut, N., Epinephrine Compound: Unveiling Its Optical And Thermochemical Properties Via Quantum Computation Methods.
- [21] Verma, P., Janesko, B.G., Wang, Y., He, X., Scalmani, G., Frisch, M.J., And Truhlar, D.G. (2019). M11plus: A Range-Separated Hybrid Meta Functional With Both Local And Rung-3.5 Correlation Terms And High Across-The-Board Accuracy For Chemical Applications, *Journal Of Chemical Theory And Computation*, 15 (9), Pp: 4804-4815.
- [22] Sucheta, M., Pramod, A.G., Zikriya, M., Salma, K.M., Venugopal, N., Chaithra, R., Harshitha, D., Amudan, S., Renuka, C.G. And Murthy, S., 2022. Frontier Molecular Orbital, Molecular Structure And Thermal Properties Of 2, 4, 6, 8-Tetramethyl-2, 3, 6, 7-Tetrahydro-S-Indacene-1, 5-Dione Using DFT Calculation. *Materials Today: Proceedings*, 62, Pp.5241-5244.
- [23] O'boyle, N.M., Tenderholt, A.L. And Langner, K.M., 2008. Cclic: A Library For Package-Independent Computational Chemistry Algorithms. *Journal Of Computational Chemistry*, 29(5), Pp.839-845.
- [24] Mohamed, H.S.H. And Ahmed, S.A., 2019. Reviewing Of Synthesis And Computational Studies Of Pyrazolo Pyrimidine Derivatives. *J Chem Rev*, 1(3), Pp.154-251.
- [25] Hammoudan, I., Aboulmouhajir, A., Dakir, M., Temsamani, D.R., Bakhouch, M., Bazi, D.E. And Chtita, S., 2023. Mechanistic Elucidation Of Diels–Alder Cycloaddition Reactions Between Quinoflavonoid And Substituted Butadiene Using LOL, ELF, QTAIM, And DFT Studies. *Structural Chemistry*, 34(3), Pp.959-969.
- [26] Johnson, E.R., Keinan, S., Mori-Sánchez, P., Contreras-García, J., Cohen, A.J. And Yang, W., 2010. Revealing Noncovalent Interactions. *Journal Of The American Chemical Society*, 132(18), Pp.6498-6506.
- [27] Akman, F., Demirpolat, A., Kazachenko, A.S., Kazachenko, A.S., Issaoui, N. And Al-Dossary, O., 2023. Molecular Structure, Electronic Properties, Reactivity (ELF, LOL, And Fukui), And NCI-RDG Studies Of The Binary Mixture Of Water And Essential Oil Of Phlomis Bruguieri. *Molecules*, 28(6), P.2684.
- [28] Domingo, L.R., Aurell, M.J., Pérez, P. And Contreras, R., 2002. Quantitative Characterization Of The Global Electrophilicity Power Of Common Diene/Dienophile Pairs In Diels–Alder Reactions. *Tetrahedron*, 58(22), Pp.4417-4423.
- [29] Macbride, D.M., Malone, C.G., Hebb, J.P. And Cravalho, E.G., 1997. Effect Of Temperature Variation On FT-IR Spectrometer Stability. *Applied Spectroscopy*, 51(1), Pp.43-50.

- [30] Ikawa, T., *Simple Arylation*, In *Comprehensive Aryne Synthetic Chemistry* 2022, Elsevier. P. 15-56.
- [31] Speight, J.G., 2016. *Environmental Organic Chemistry For Engineers*. Butterworth-Heinemann.
- [32] Gupta, V., (2015). *Principles And Applications Of Quantum Chemistry*, Academic Press,
- [33] Ouellette, R.J. And Rawn, J.D., (2015). *Principles Of Organic Chemistry*, Academic Press,
- [34] MAMAND, D., 2019. Theoretical Calculations And Spectroscopic Analysis Of Gaussian Computational Examination-NMR, FTIR, UV-Visible, MEP On 2, 4, 6-Nitrophenol. *Journal Of Physical Chemistry And Functional Materials*, 2(2), Pp.77-86.
- [35] Croker, E.L. And Basu-Dutt, S., 2002. A Classical And Quantum Chemical Analysis Of Gaseous Heat Capacity. *The Chemical Educator*, 7(3), Pp.136-141.
- [36] Vijjapu, R. And Tiwari, S., 2022. Thermodynamics Of Sensible Thermal Energy Storage Systems.
- [37] López-Chávez, E., Cruz-Torres, A., De Landa Castillo-Alvarado, F., Ortiz-López, J., Peña-Castañeda, Y.A. And Martínez-Magadán, J.M., 2011. Vibrational Analysis And Thermodynamic Properties Of C 120 Nanotorus: A DFT Study. *Journal Of Nanoparticle Research*, 13, Pp.6649-6659.
- [38] Parlak, A.E., Omar, R.A., Koparir, P. And Salih, M.I., 2022. Experimental, DFT And Theoretical Corrosion Study For 4-(((4-Ethyl-5-(Thiophen-2-Yl)-4H-1, 2, 4-Triazole-3-Yl) Thio) Methyl)-7, 8-Dimethyl-2H-Chromen-2-One. *Arabian Journal Of Chemistry*, 15(9), P.104088.
- [39] Korkmaz, A.A., Ahmed, L.O., Kareem, R.O., Kebiroglu, H., Ates, T., Bulut, N., Kaygili, O. And Ates, B., 2022. Theoretical And Experimental Characterization Of Sn-Based Hydroxyapatites Doped With Bi. *Journal Of The Australian Ceramic Society*, 58(3), Pp.803-815.
- [40] Kareem, R.O., Kaygili, O., Ates, T., Bulut, N., Koytepe, S., Kuruçay, A., Ercan, F. And Ercan, I., 2022. Experimental And Theoretical Characterization Of Bi-Based Hydroxyapatites Doped With Ce. *Ceramics International*, 48(22), Pp.33440-33454.
- [41] İsen, F., Kaygili, O., Bulut, N., Ates, T., Osmanlioğlu, F., Keser, S., Tatar, B., Özcan, İ., Ates, B., Ercan, F. And Ercan, I., 2023. Experimental And Theoretical Characterization Of Dy-Doped Hydroxyapatites. *Journal Of The Australian Ceramic Society*, Pp.1-16.
- [42] Kareem, R.O., 2023. Synthesis And Characterization Of Bismuth-Based Hydroxyapatites Doped With Cerium.
- [43] Kamel, M. And Mohammadifard, K., 2021. Thermodynamic And Reactivity Descriptors Studies On The Interaction Of Flutamide Anticancer Drug With Nucleobases: A Computational View. *Chemical Review And Letters*, 4(1), Pp.54-65.
- [44] Kareem, R.O., Kebiroğlu, M.H., Hamad, O.A., Kaygili, O. And Bulut, N., Epinephrine Compound: Unveiling Its Optical And Thermochemical Properties Via Quantum Computation Methods 2024.
- [45] Shahab, H. And Husain, Y., 2021. Theoretical Study For Chemical Reactivity Descriptors Of Tetrathiafulvalene In Gas Phase And Solvent Phases Based On Density Functional Theory. *Passer Journal Of Basic And Applied Sciences*, 3(2), Pp.167-173.
- [46] Mustafa, M.D. And Mohammad, Q.H., 2023. Quantum Chemical And Monte Carlo Simulations On Corrosion Inhibition Efficiency Of 2-Mercapto-5-Phenylfuran And Bis (Pyridyl) Oxadiazoles. *Известия Высших Учебных Заведений. Химия И Химическая Технология*, 66(8), Pp.33-45.